ACS APPLIED MATERIALS & INTERFACES

Research Article

www.acsami.org

Core–Shell Nanoparticles Based on Pullulan and Poly(β-amino) Ester for Hepatoma-Targeted Codelivery of Gene and Chemotherapy Agent

Yuanyuan Liu,[†,§] Yan Wang,[†,§] Cong Zhang,[†] Ping Zhou,[†] Yang Liu,[†] Tong An,[†] Duxin Sun,[‡] Ning Zhang,*[,†] and Yinsong Wang*[,†]

[†]Tianjin Cancer Institute and Hospital, Laboratory of Breast Cancer Prevention and Therapy, Ministry of Education, Research Center of Basic Medical Science & School of Pharmacy, Tianjin Key Laboratory on Technologies Enabling Development of Clinical Therapeutics and Diagnostics (Theranostics), Tianjin Medical University, No. 22 Qixiangtai Road, Heping District, Tianjin 300070, People's Republic of China

[‡]Department of Pharmaceutical Sciences, College of Pharmacy, University of Michigan, Ann Arbor, Michigan 48109, United States

Supporting Information

ABSTRACT: This study designs a novel nanoparticle system with core–shell structure based on pullulan and poly(β-amino) ester (PBAE) for the hepatoma-targeted codelivery of gene and chemotherapy agent. Plasmid DNA expressing green fluorescent protein (pEGFP), as a model gene, was fully condensed with cationic PBAE to form the inner core of PBAE/pEGFP polycomplex. Methotrexate (MTX), as a model chemotherapy agent, was conjugated to pullulan by ester bond to synthesize polymeric prodrug of MTX-PL. MTX-PL was then adsorbed on the surface of PBAE/pEGFP polycomplex to form MTX-PL/PBAE/pEGFP nanoparticles with a classic core–shell structure. MTX-PL was also used as a hepatoma targeting moiety, because of its specific binding affinity for asialoglycoprotein receptor (ASGPR) overexpressed by human hepatoma HepG2 cells. MTX-PL/PBAE/pEGFP nanoparticles realized the efficient transfection of pEGFP in HepG2 cells and exhibited significant inhibitory effect on the cell proliferation. In HepG2 tumor-bearing nude mice, MTX-PL/PBAE/pEGFP nanoparticles were mainly distributed in the tumor after 24 h postintravenous injection. Altogether, this novel codelivery system with a strong hepatoma-targeting property achieved simultaneous delivery of gene and chemotherapy agent into tumor at both cellular and animal levels.

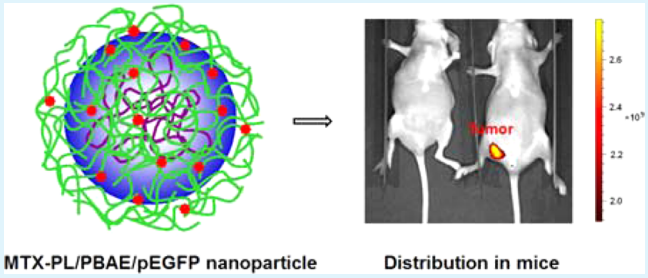

KEYWORDS: *pullulan, poly(β-amino) ester, hepatoma, gene, chemotherapy agent*

INTRODUCTION

Hepatocellular carcinoma (HCC) is the third leading cause of cancer mortality worldwide, with the highest incidence rate reported in East Asia.[1,2] Surgical removal is believed as the optimal treatment for HCC, but most patients are diagnosed already at an advanced stage and are not suitable for hepatectomy. Traditional treatments, including chemotherapy and radiotherapy, have not been found to be effective in prolonging overall survival and often cause side effects.[3−6] Hence, exploring effective therapies against HCC is of great urgency and attracts wide attention in medical and pharmaceutical field. Increasing investigations have confirmed that the tumorigenesis and metastasis of HCC are a multigene-involving and multistep process; thus, gene therapy is currently believed to be a potent strategy for HCC treatments. In addition, combined gene therapy and chemotherapy often exhibit synergic effects on HCC[7−10] and are hoped to be an effective method in clinical practice.[11,12]

One of the main challenges in advancing gene therapy technology is its effective delivery. Many viral vectors have been successfully used for ex vivo gene therapy, but their applications in vivo are greatly limited because of some intrinsic drawbacks, including the immunogenicity, low loading capacity for gene, and difficulty in mass production.[13,14] Nonviral vectors are therefore increasingly focused on because of their enhanced biosafety and biocompatibility.[15−17] A large number of cationic polymers have been reported to be capable of delivering genes.[18−20] Poly(β-amino) esters (PBAEs), first developed by the Langer group, exhibit great potential as gene delivery reagents because they are easily synthesized and exhibit the relatively low toxicities and high transfection efficiencies in a wide variety of cell types. PBAEs exhibit high efficiency of gene transfection because they can carry DNA to enter cells through endocytosis and then successfully escape from endosomal/lysosomal compartment by the proton sponge effect. Thus, gene carriers based on PBAEs have attracted increased attentions recently.[21−25]

Pullulan is a water-soluble, nontoxic, and nonimmunogenic nature polysaccharide that is produced by *Aureobasidium*

Received: July 1, 2014
Accepted: October 7, 2014
Published: October 7, 2014

   dx.doi.org/10.1021/am504203x | ACS Appl. Mater. Interfaces 2014, 6, 18712−18720

Scheme 1. Chemical Structures of PBAE (a) and MTX-PL Conjugate (b) and the Preparation Illustration of MTX-PL/PBAE/pEGFP Nanoparticles (c)

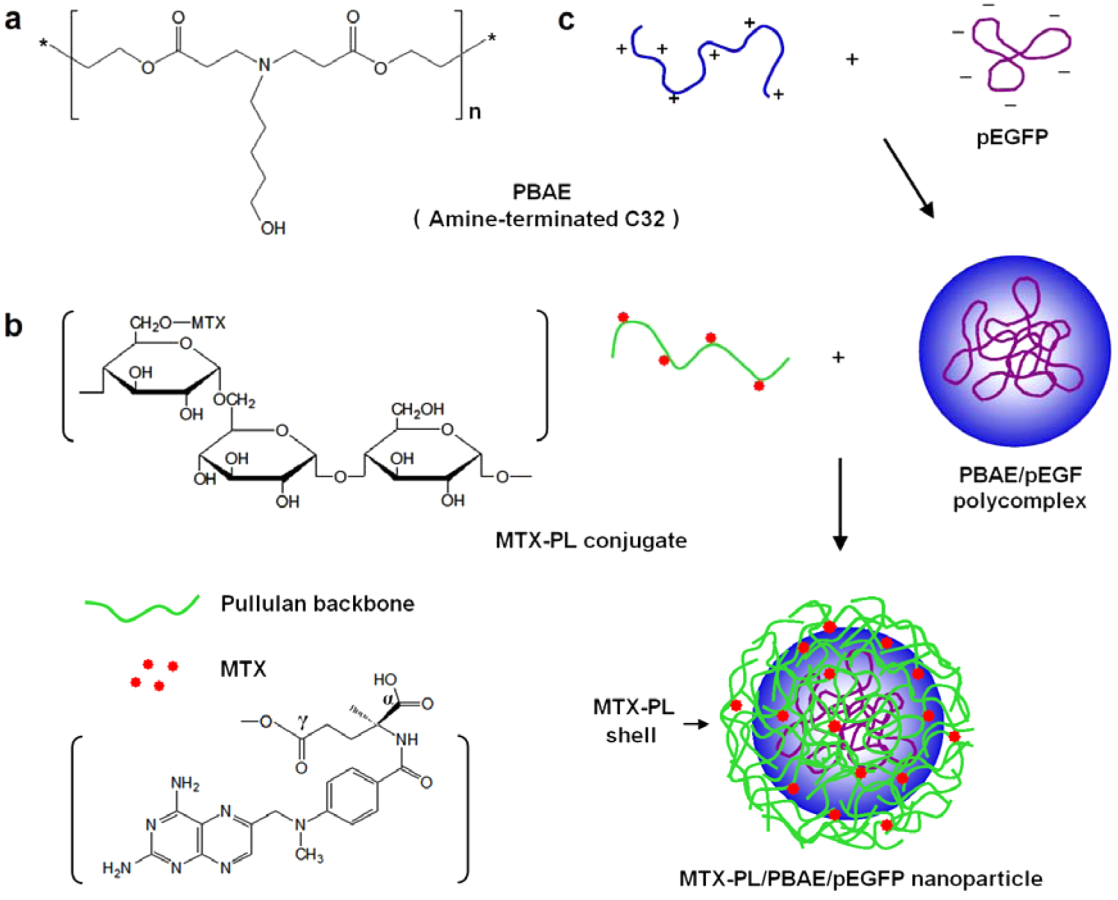

pullulans. Because of its excellent biological and physicochemical features, pullulan has become an attractive ingredient for many pharmaceutical applications and chemical manipulations.[26,27] Some investigations have shown that pullulan has a prolonged circulation time in blood due to its electric neutrality[28] and a liver-targeting capability because of its high affinity for the asialoglycoprotein receptor (ASGPR).[29] In our previous reports, several pullulan-based carriers were prepared and used for hepatoma-targeted delivery of chemotherapy agents. Some of them exhibited the potential as drug carriers for the treatment of HCC.[30,31]

In this study, we designed a novel nanoparticle system for the heptoma-targeted codelivery of gene and chemotherapy agent using pullulan and PBAE as the carrier materials. Scheme 1 illustrates the structure of this nanoparticle carrier. Plasmid DNA expressing green fluorescent protein (pEGFP), as a model gene, was first condensed with cationic PBAE to form the inner core of PBAE/pEGFP polycomplex. Chemotherapy agent methotrexate (MTX) was conjugated to pullulan via ester bond to synthesize polymeric prodrug of MTX-PL. Next, MTX-PL was coated on the surface of PBAE/pEGFP polycomplex by adsorption to form MTX-PL/PBAE/pEGFP nanoparticle with a classic core−shell structure, thus realizing coloading of pEGFP and MTX. In order to evaluate the potential of this novel codelivery system for combination of gene therapy and chemotherapy, we investigated the transfection efficiency and cytotoxicity of MTX-PL/PBAE/pEGFP nanoparticles in human hepatoma HepG2 cells and further assessed their hepatoma-targeted delivery in HepG2 tumor-bearing nude mice.

EXPERIMENTAL SECTION

Chemicals. Amine-terminated PBAE C32 was synthesized by Michael-addition reaction of 5-amino-1-pentanol and 1,4-butanediol diacrylate according to previous reports.[22,25] The synthesis and characterization of PBAE are described in detailed in the Supporting Information. pEGFP was amplified in Recombinant *Escherichia coli* (*E. coli*) DH5-α and purified with a Qiagen's Giga-Prep kit (Valencia, CA, USA). Pullulan (molecular mass of 200 kDa) was purchased from Hayashibara Biochemical Laboratory, Inc. (Okayama, Japan). MTX was obtained from Huzhou Zhanwang Pharmaceutical Co. Ltd. (Zhejiang, Chnia). Branched polyethylenimine (PEI, MW = 25 kDa), bovine serum albumin (BSA), dicyclohexylcarbodiimide (DCC), 4-(dimethylamino)pyridine (DMAP), dimethyl sulfoxide (DMSO, dry grade), and fluorescein 5-isothiocyanate (FITC) were purchased from Sigma-Aldrich Co. (St. Loius, MO, USA). Sodium cyanoborohydride ($NaCNBH_3$) was purchased from Fluka (Deisenhofen, Germany). Cy5.5 NHS ester was purchased from Fanbo Biochemicals (Beijing, China). Cell counting kit-8 (CCK-8) was purchased from Dojindo (Beijing, China). All other chemical reagents were analytical grade and obtained from commercial sources.

Cells and Animals. Human normal liver HL-7702 cells and hepatoma HepG2 cells, obtained from American Type Culture Collection, were cultured in Dulbecco's modified Eagle medium (Invitrogen) containing 10 v/v % fetal bovine serum (FBS, Sigma-Aldrich) and 1 v/v % penicillin/streptomycin (Sigma-Aldrich) at 37 °C in an atmosphere of 5% CO_2. The Balb/c nude mice were bought from Wei Tong Li Hua Experimental Animal Co. (Beijing, China). A xenograft model of HCC was established by subcutaneous injection of HepG2 cells into nude mice as described previously,[32] and the experimental protocol was approved by the Tianjin Medical University Animal Care and Use Committee.

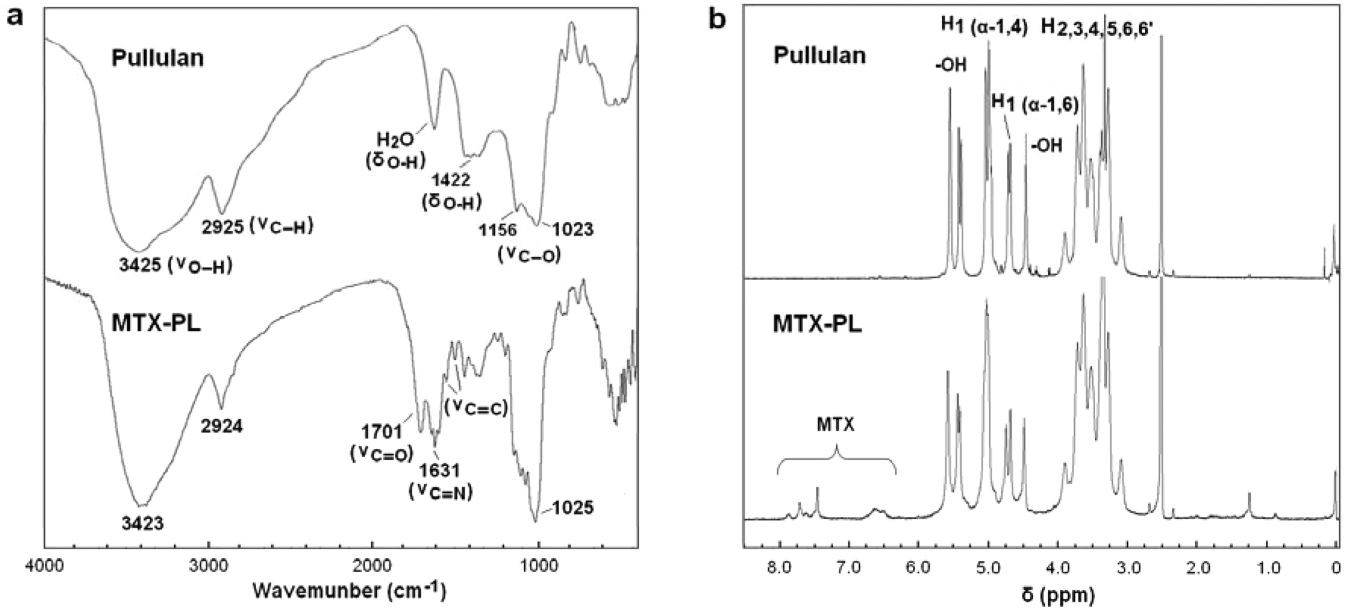

Figure 1. IR (a) and ^{1}H NMR spectra (b) of pullulan and MTX-PL.

Synthesis and Characterization of MTX-PL. MTX was conjugated to pullulan through esterification under DCC/DMAP catalysis according to our previous method.[31] Briefly, 0.2 g of MTX was dissolved in dried DMSO and activated by reaction with DCC/DMAP (1.0 equiv) for 2 h. Then 0.5 g of pullulan was added and the mixture was stirred for 72 h at room temperature with avoidance of light. After reaction, the dicyclohexylurea precipitate was removed by the filtration. The filtrate was dialyzed against deionized water for 48 h with six exchanges and subsequently dried by freeze-drying to obtain polymeric prodrug of MTX-PL. IR spectra of pullulan and MTX-PL were measured on a FT-IR spectrometer (Nicolet NEXUS 470-ESP, USA) using KBr pellets. ^{1}H NMR spectra were recorded on a 500 MHz proton nuclear magnetic resonance (Varian INOVA, USA) using DMSO-d_6 as the solvent. MTX content of MTX-PL was measured using an ultraviolet (UV) spectrophotometer (BCKMAN DUR 640, USA) at 306 nm. In addition, MTX-PL was labeled with FITC to form MTX-PL-FITC according to the method presented in our previous study.[31]

Preparation of Lactosylated BSA (LacBSA). LacBSA was prepared by coupling lactose to ε-NH_2 of lysine residues of BSA under the reduction of sodium cyanoborohydride. In brief, 150 mg of BSA and 350 mg of lactose were dissolved in PBS solution (pH 7.0) containing 0.02% NaN_3, and the mixture was then stirred for 2 h at room temperature. After that, 500 mg of $NaCNBH_3$ was added and subsequently stirred for 72 h at 37 °C. Next, the reactant mixture was dialyzed and freeze-dried to obtain LacBSA.

Ligand Competition Binding Assay. Ligand competition binding assay was used to evaluate the binding affinity of MTX-PL-FITC for ASGPR that overexpressed in HepG2 cells. Briefly, HepG2 cells were seeded at a density of 5×10^4 cells/well in glass bottom cell culture dish. LacBSA was added at different concentrations and then incubated for 1 h. Next, MTX-PL-FITC was respectively added to the above dishes at MTX-PL-FITC/LacBSA weight ratios of 1/80, 1/50, 1/30, 1/10, and 1/0. After continuous incubation for 8 h, cells were washed three times with PBS and incubated with culture medium containing Hoechst 33342 for 15 min to visualize cell nucleus. After that, cells were washed twice with cold PBS and then dispersed in the fresh medium. Finally, cells were observed under Leica TCS SP5 confocal microscope (Mannhein, Germany) and analyzed by a FACS Calibur flow cytometer (Becton Dickinson, San Jose, CA, USA).

Preparation and Characterization of PBAE/pEGFP Polycomplexes. pEGFP was condensed with cationic PBAE to form PBAE/pEGFP polycomplexes with different PBAE/pEGFP weight ratios. Briefly, PBAE was dissolved in 50 μL of 25 mM sodium acetate buffer (pH 5.2) at various concentrations. Then 50 μL of pEGFP (40 μg/mL) was added to the above PBAE solutions. All mixtures were vortexed for 30 s and further incubated for 20 min to allow complex formation. The size and ζ potential of resultant PBAE/pEGFP polycomplex were determined by particle size and ζ potential analyzer (Zetasizer Nano-ZS, Malvern Instruments, Ltd., United Kingdom), and their morphologies were observed using transmission electron microscope (TEM, Tecnai G2 20S-Twin, USA).

Electrophoretic Mobility Shift Assay of PBAE/pEGFP Polycomplexes. The ability of PBAE to condense plasmid DNA was assessed by the agarose gel electrophoresis. In brief, an amount of 10 μL of the above PBAE/pEGFP polycomplex solutions (about 0.2 μg of plasmid DNA) was loaded on a 1% agarose gel containing 0.5 μg/mL ethidium bromide (EB). Electrophoresis was carried out in 1× TAE buffer (40 mM Tris, 20 mM acetate, 2 mM EDTA, pH 8.1) at 100 V with JUNYI-SPAT electrophoresis apparatus (Beijing Junyi-Dongfang, China) for about 30 min. DNA bands were imaged using a GelDoc-ItTM imaging system (UVP Inc., America).

Surface Coating of PBAE/pEGFP Polycomplex with MTX-PL. MTX-PL was coated on the surface of PBAE/pEGFP polycomplexe at different MTX-PL/PBAE/pEGFP weight ratios (10/50/1, 20/50/1, and 30/50/1) by the adsorption method. Typically, 10 μL of MTX-PL in DMSO was added to PBAE/pEGFP polycomplex solution under gentle vortexing followed by shaking for 4 h at 4 °C. MTX-PL/PBAE/pEGFP nanoparticles were thus produced and subsequently characterized using Zetasizer Nano-ZS and TEM. In addition, pullulan-surface adsorbed PBAE/pEGFP (PL/PBAE/pEGFP) nanoparticles were also prepared as the control.

In Vitro Transfection Assay. Human hepatoma HepG2 cells were grown in 24-well plates in 500 μL of culture medium at an initial seeding density of 7.5×10^4 cells/well. After incubation for 24 h, the culture medium was removed and replaced with 500 μL of serum-free culture medium containing PBAE/pEGFP polycomplexes or MTX-PL/PBAE/pEGFP nanoparticles with varying weight ratios. After a further 4 h incubation, the serum-free culture medium was removed and replaced with 500 μL of fresh culture medium containing 10% FBS. Cells were incubated for an additional 48 h and then visualized with an automated inverted fluorescence microscope (Olympus IX71, Tokyo, Japan) for observing EGFP expressions. To determine the transfection efficiencies, cells were harvested by trypsinization, washed with phosphate buffered saline (PBS), and finally analyzed by a FACS Calibur flow cytometer (Becton Dickinson, San Jose, CA, USA).

Cell Viability Assay. CCK8 assay was used to evaluate the in vitro cytotoxicities of PBAE/pEGFP polycomplex, MTX-PL/PBAE/pEGFP and PL/PBAE/pEGFP nanoparticles in HL-7702 and HepG2 cells.

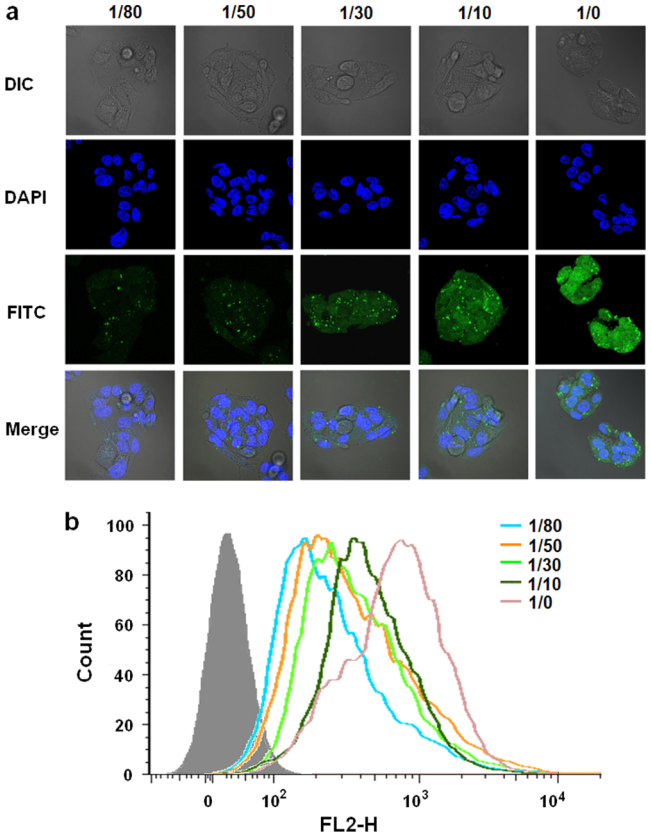

Figure 2. Confocal images (a) and flow cytometric analysis (b) of HepG2 cells incubated with LacBSA and MTX-PL-FITC at different MTX-PL-FITC/LacBSA weight ratios.

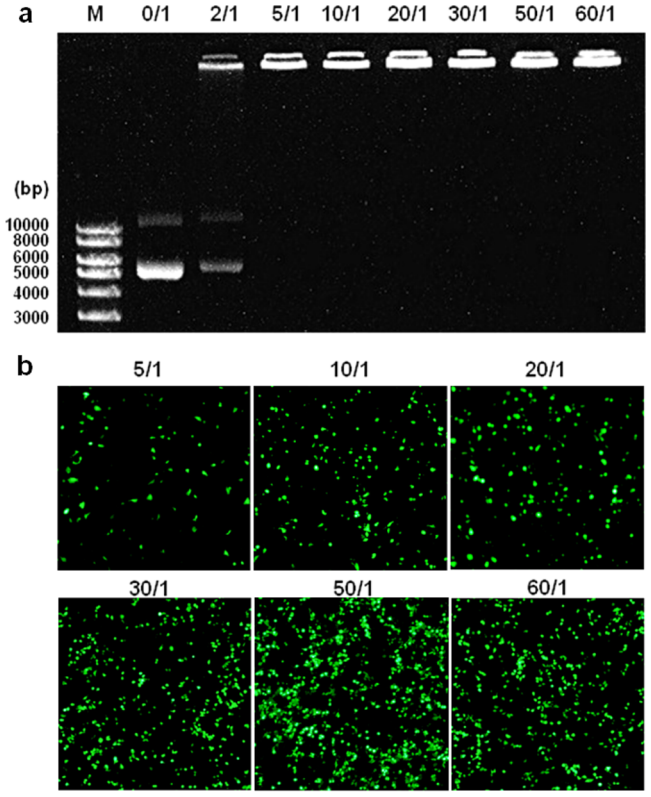

Figure 3. Electrophoretic mobility shift assays of PBAE/pEGFP polycomplexes with different weight ratios (a) and fluorescent images of EGFP expressions in HepG2 cells mediated by PBAE/pEGFP polycomplexes (b).

Briefly, cells were cultured in the 96-well plate with a seeding density of 5000 cells/well for 24 h. Then the culture medium was removed and replaced with fresh culture medium containing PBAE/pEGFP polycomplex, MTX-PL/PBAE/pEGFP, or PL/PBAE/pEGFP nanoparticles with different pEGFP concentrations and then continuously incubated for 72 h. After that, 200 μL of fresh medium containing 20 μL of CCK reagent was added to each well and incubated for an additional 2 h. Next, the plate was shaken for 300 s and the absorbance was measured at 570 nm using an ELX800 absorbance microplate reader (Biotek EPOCH, Winooski, VT, USA) to calculate the cell survival rate.

In Vivo Imaging Analysis. MTX-PL was labeled with a near-IR dye, Cy5.5, for in vivo imaging. Briefly, MTX-PL and Cy5.5 NHS ester were dissolved in dried DMSO and reacted for 72 h at room temperature by avoiding light. Excess dye molecules were removed by centrifugation filtration through 3 kDa MWCO Amicon filters (Millipore, Billerica, MA, USA) and washed with water over 8 times. Cy5.5 labeled MTX-PL (MTX-PL-Cy5.5) was then coated on the surface of PBAE/pEGFP polycomplex to prepare MTX-PL-Cy5.5/PBAE/pEGFP nanoparticles with MTX-PL/PBAE/pEGFP weight ratio of 20/50/10. Next, HepG2 tumor-bearing nude mice were intravenously injected with 100 μL of MTX-PL-Cy5.5 and MTX-PL-Cy5.5/PBAE/pEGFP nanoparticle solutions and then imaged using Maestro in vivo imaging system (CRi, Woburn, MA, USA) at predefined times. All mice were sacrificed at 24 h after injection, and the major organs, including liver, spleen, kidney, heart, lung, and tumor, were collected for further detection.

Statistical Analysis. Each experiment was repeated three times, and all data were expressed as the mean ± standard deviation. Statistical analysis was performed using analysis of variance (ANOVA), and $p < 0.05$ was considered statistically significant.

RESULTS AND DISCUSSION

MTX, as a model chemotherapy agent, was conjugated to pullulan via ester bond between γ-carboxyl group of MTX and hydroxyl group of pullulan (Scheme 1). Figure 1 shows FT-IR and ^{1}H NMR spectra of pullulan and MTX-PL. As compared with pullulan, the IR signals of MTX-PL at 1701, 1631, 1560, and 1509 cm^{-1} were respectively assigned to the stretching vibrations of −C═O, −C═N, and aromatic −C═C− in MTX moiety, and the intensity of hydroxyl stretching at 3423 cm^{-1} obviously decreased because of the esterization reaction between pullulan with MTX (Figure 1a). The proton peaks of the sugar unit were assigned in the ^{1}HNMR spectrum of pullulan, and the characteristic proton peaks of benzene and pterin rings of MTX moiety in MTX-PL appeared in the chemical-shift range of 6.3−8.0 ppm (Figure 1b). All of the above results confirmed that MTX was successfully conjugated to pullulan via ester bond. MTX content, determined by UV method at 306 nm, was 15.2% when the feed weight ratio of MTX to pullulan was 2/5 in synthesis of MTX-PL.

ASGPR is overexpressed in hepatocytes and hepatoma cells and can transport large molecules across cell membranes to enter cells. Thus, ASGPR-mediated endocytosis is believed as an effective strategy for hepatoma-targeting drug delivery.[33−35] Some investigations have reported that pullulan is a specific ligand of ASGPR,[29] and our previous studies have realized liver- or hepatoma-targeting delivery of chemotherapeutic agents using pullulan-based carriers.[30,31] In this study, polymeric prodrug of MTX-PL was synthesized and used as a hepatoma-targeting material. The specific binding affinity of MTX-PL for ASGPR was assessed using ligand competition binding assay. HepG2 cells were first incubated with LacBSA, a known ligand of ASGPR,[36] at different concentrations, and MTX-PL-FITC was then added to compete with LacBSA for binding to ASGPR.

dx.doi.org/10.1021/am504203x | ACS Appl. Mater. Interfaces 2014, 6, 18712−18720

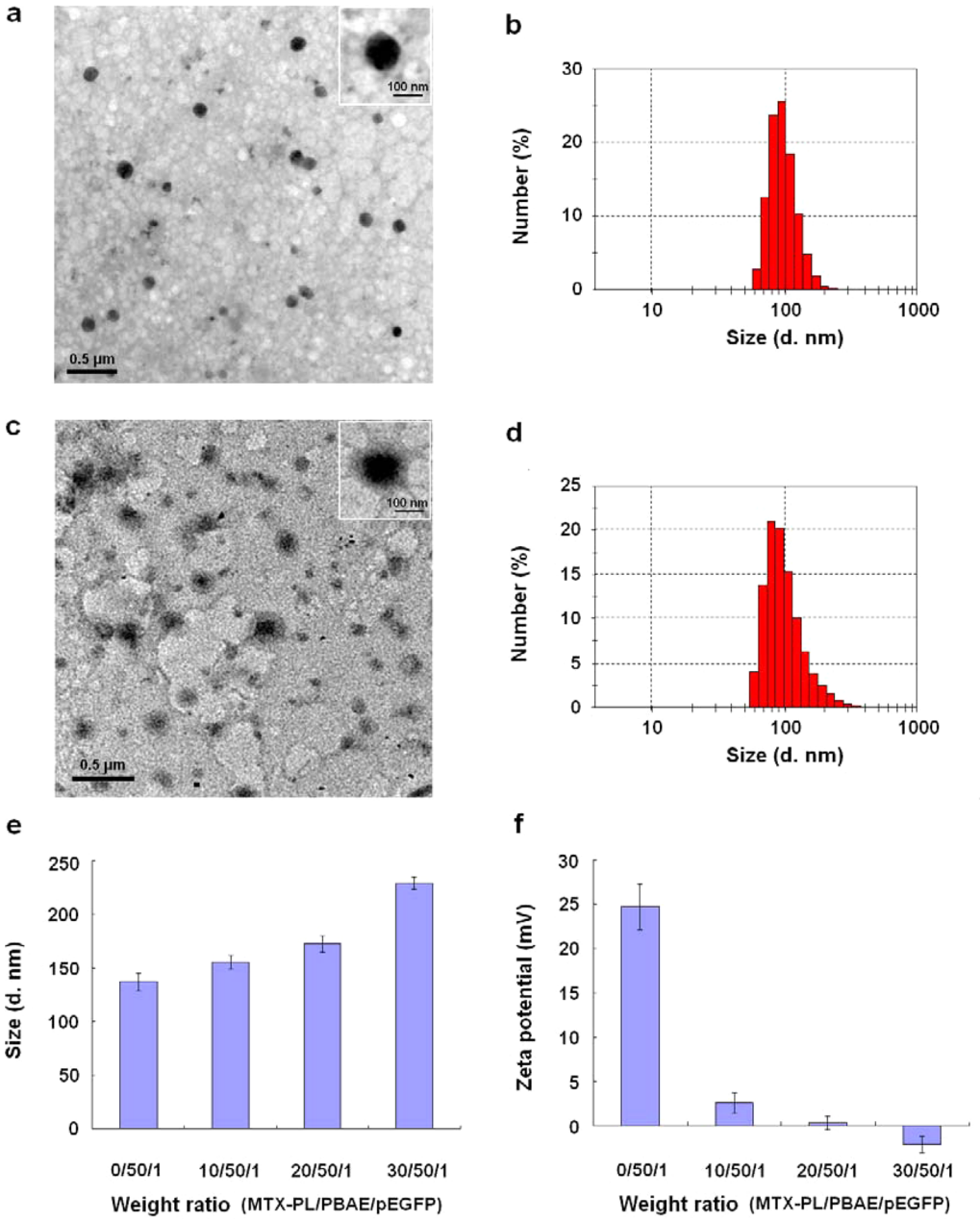

Figure 4. Morphological observations and size determinations of PBAE/pEGFP polycomplex and MTX-PL/PBAE/pEGFP nanoparticles. TEM images (a) and size distribution (b) of PBAE/pEGFP polycomplex with PBAE/pEGFP weight ratio of 50/1. TEM image (c) and size distribution (d) of MTX-PL/PBAE/pEGFP nanoparticles with MTX-PL/PBAE/pEGFP weight ratio of 20/50/1. Sizes (e) and the ζ potentials (f) of MTX-PL/PBAE/pEGFP nanoparticles with different MTX-PL/PBAE/pEGFP weight ratios.

As shown in Figure 2, the increased fluorescence intensity of MTX-PL-FITC in HepG2 cells with increasing ratios of MTX-PL-FITC/LacBSA was evidently observed by both confocal microscopy observation (Figure 2a) and flow cytometric analysis (Figure 2b). As LacBSA could specifically bind to ASGPR, it could be deduced that MTX-PL-FITC entered HepG2 cells mainly by ASGPR-mediated endocytosis and had potential as a hepatoma-targeting carrier material. In addition, MTX-PL-FITC was mainly distributed in the cytoplasm at low MTX-PL-FITC/LacBSA weight ratio but gradually entered cell nucleus with MTX-PL-FITC/LacBSA weight ratio increasing, which was conducive to the intracellular transport of genes.

PBAEs, as a novel class of cationic polymers, exhibit comparable or even higher transfection efficiencies with much lower toxicity compared to polyethelenimine (PEI).[21−25] Amine-terminated C32 (Scheme 1) was an effective transfection reagent and has been widely studied for the transfections of various genes.[22,25] In this study, amine-terminated C32 was synthesized (Supporting Information) and applied as the transfection vector for pEGFP. We first assessed its ability to condense pEGFP by the electrophoretic mobility shift assay. As shown in Figure 3a, PBAE could completely inhibit pEGFP migration when PBAE/pEGFP weight ratio was higher than 5/1, indicating that PBAE had a good capability of condensing pEGFP to form stable polycomplex. At the same time, the transfection efficiency of PBAE/pEGFP polycomplex was evaluated in HepG2 cells using the fluorescence microscope. As shown in Figure 3b, the fluorescence intensity of EGFP expression in HepG2 cells increased

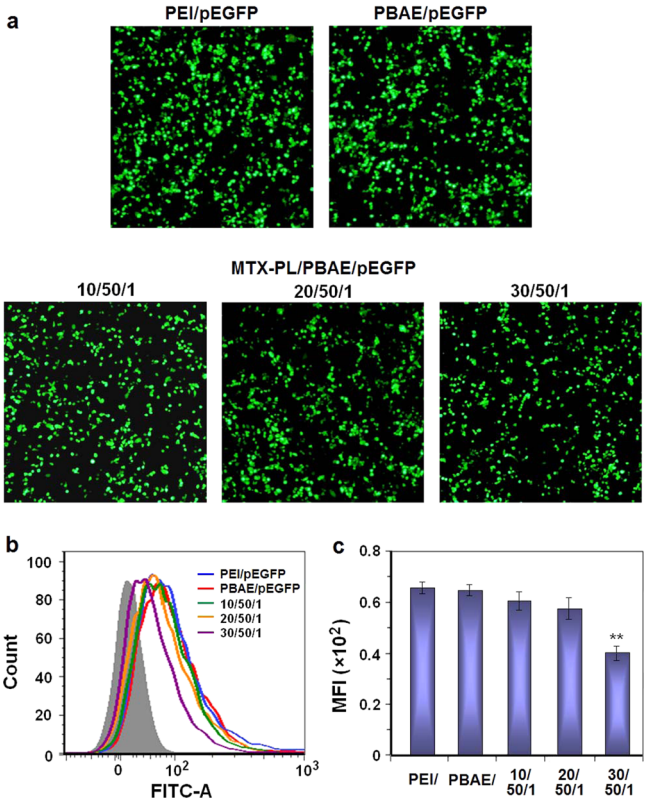

Figure 5. EGFP expressions mediated by PEI/pEGFP complex, PBAE/pEGFP polycomplex, and MTX-PL/PBAE/pEGFP nanoparticles with different MTX-PL/PBAE/pEGFP weight ratios: (a) fluorescence images; (b) profiles assayed by flow cytometry; (c) comparison of MFI values from the flow cytometry profiles (mean ± SD; $n = 3$; **, $p < 0.05$).

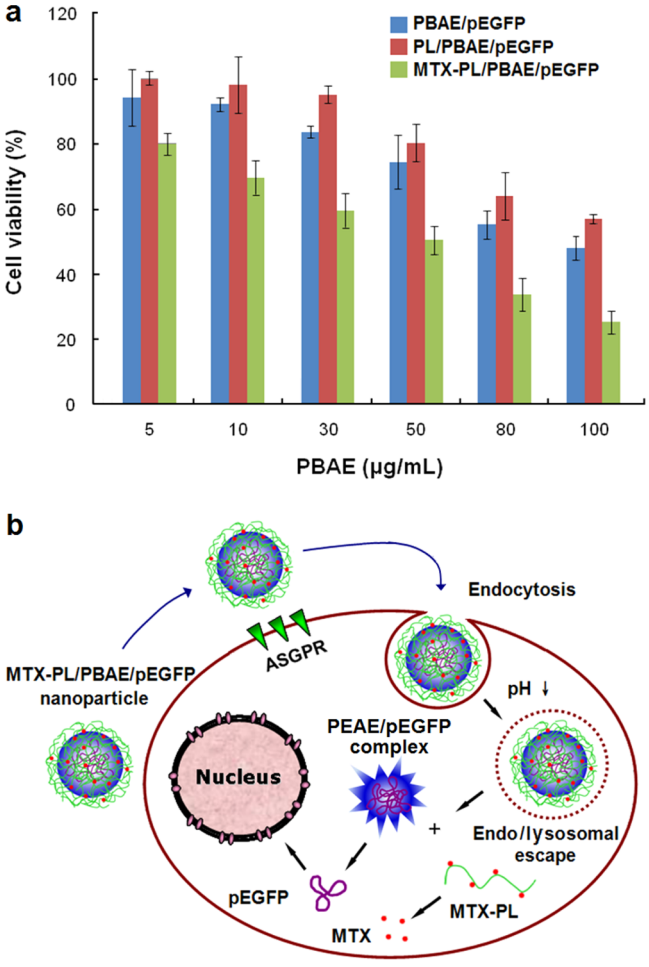

Figure 6. Inhibitory effects of PBAE/pEGFP polycomplex, PL/PBAE/pEGFP, and MTX-PL/PBAE/pEGFP nanoparticles on the proliferations of HepG2 cells (a) and illustration of intracellular delivery of MTX-PL/PBAE/pEGFP nanoparticles (b).

with PBAE/pEGFP weight ratio increasing from 5/1 to 50/1 but subsequently decreased with PBAE/pEGFP weight ratio further increasing. Thus, 50/1 was believed to be an optimal PBAE/pEGFP weight ratio to transfect pEGFP in HepG2 cells and used in our following experiments.

To realize the hepatoma-targeted delivery of PBAE/pEGFP polycomplex, MTX-PL was coated on its surface by adsorption method (Scheme 1). Figure 4 shows the TEM images and size distributions of PBAE/pEGFP polycomplex and MTX-PL/PBAE/pEGFP nanoparticles. PBAE/pEGFP polycomplex with PBAE/pEGFP weight ratio of 50/1 exhibited spherical shape (Figure 4a), and its size was 137.4 ± 8.9 nm with a relatively narrow distribution (Figure 4b). MTX-PL/PBAE/pEGFP nanoparticles with MTX-PL/PBAE/pEGFP weight ratio of 20/50/1 maintained spherical shapes and had a classic core−shell structure in which polysaccharide shells with a thickness of 20−50 nm were evidently observed (Figure 4c). Their size was 172.9 ± 6.5 nm with a slightly broad size distribution. Compared to PBAE/pEGFP polycomplex, MTX-PL/PBAE/pEGFP nanoparticles had evidently larger sizes and their size increased from 155.6 to 229.2 nm with the increase of MTX-PL/PBAE/pEGFP weight ratio (Figure 4e). Moreover, the ζ potential of PBAE/pEGFP polycomplex was +24.69 mV, but the ζ potentials of MTX-PL/PBAE/pEGFP nanoparticles were 2.61, 0.39, and −2.08 mV, respectively corresponding to MTX-PL/PBAE/pEGFP weight ratios of 10/50/1, 20/50/1 and 30/50/1 (Figure 4f). All of the above results confirmed that MTX-PL was successfully coated on the surface of PBAE/pEGFP polycomplex and the thicker polysaccharide shells were formed when the MTX-PL/PBAE/pEGFP weight ratio increased during the process of surface modification.

In order to evaluate the influence of MTX-PL surface modification on the in vitro transfection of PBAE/pEGFP polycomplex, we qualitatively and quantitatively analyzed the transfection efficiencies of MTX-PL/PBAE/pEGFP nanoparticles in HepG2 cells respectively using the fluorescence microscopy and the flow cytometry. As shown in Figure 5a, EGFP expressions at relatively high levels in HepG2 cells were clearly observed at MTX-PL/PBAE/pEGFP weight ratios of 10/50/1, 20/50/1, and 30/50/1. The results of flow cytometric analysis including the fluorescence profiles (Figure 5b) and the comparison of median fluorescent intensities (MFI, Figure 5c) further indicated that the transfection efficiencies of MTX-PL/PBAE/pEGFP nanoparticles with MTX-PL/PBAE/pEGFP weight ratios of 10/50/1 and 20/50/1 were comparable to those of PEI/pEGFP and PBAE/pEGFP polycomplexes but evidently decreased when MTX-PL/PBAE/pEGFP weight ratio increased to 30/50/1. As described above, MTX-PL/PBAE/pEGFP nanoparticles with the larger size and the thicker polysaccharide shells were formed when the MTX-PL/PBAE/pEGFP weight ratio increased. We therefore deduced that MTX-PL/PBAE/pEGFP nanoparticles with high MTX-PL/PBAE/pEGFP weight ratio perhaps inhibited the intracellular release of PBAE/pEGFP polycomplex to a certain extent after cell

dx.doi.org/10.1021/am504203x | ACS Appl. Mater. Interfaces 2014, 6, 18712−18720

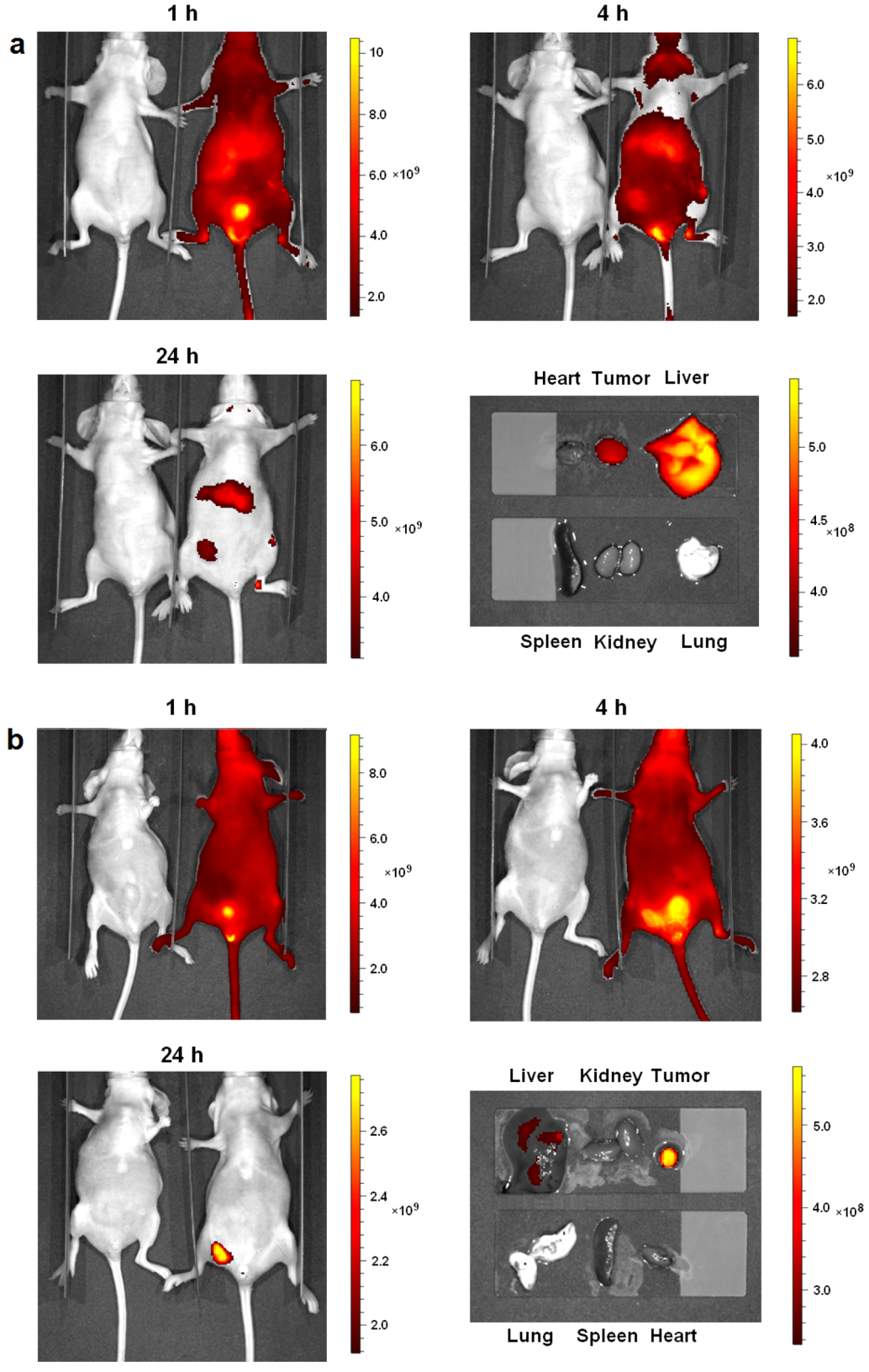

Figure 7. In vivo distributions of MTX-Cy5.5 (a) and MTX-PL-CY5.5/PBAE/pEGFP nanoparticles (b) in HeG2 tumor-bearing mice (right) at 1, 4, and 24 h after administration. The normal nude mice with injections of physiological saline (left) were used as the controls.

internalization and further influenced the transfection of pEGFP. On the basis of a balanced consideration of application essentials, e.g., the small size, the high drug loading content, and the efficient gene thransfection, 20/50/1 was believed to be an optimal MTX-PL/PBAE/pEGFP weight ratio and used in the following experiments.

It is well-known that cationic polymers can interact with negatively charged cellular membranes and thus enhance the

cellular uptake of genes. This strong interaction can usually induce high cytotoxicity due to the cellular membrane damage.[37,38] In this study, the cytotoxicity of PBAE/pEGFP polycomplex with PBAE/pEGFP weight ratio of 50/1 was first assessed by CCK-8 assay. After incubation for 48 h, PBAE/pEGFP polycomplex inhibited the proliferation of HepG2 cells in a concentration-dependent manner and exhibited a relatively low level of cytotoxicity, e.g., nearly 50% of the cells survived when PBAE concentration was up to 100 μg/mL (Figure 6a). MTX-PL, as a polymeric prodrug, was coated on the surface of PBAE/pEGFP polycomplex, thus gene therapy and chemotherapy could be effectively combined. The above results had confirmed the successful transfection of MTX-PL/PBAE/pEGFP nanoparticles in HepG2 cells. Next, we further assessed the cytotoxicity of MTX-PL/PBAE/pEGFP nanoparticles with weight ratio of 20/50/1 to preliminarily evaluate the synergistic effects of gene therapy and chemotherapy. At the same time, pullulan-surface modified PBAE/pEGFP (PL/PBAE/pEGFP) nanoparticles with the same weight ratio were also prepared as the control. As shown Figure 6a, PL/PBAE/pEGFP nanoparticles showed a slightly lower cytotoxicity than that of PBAE/pEGFP polycomplex, indicating that pullulan-surface modification was beneficial to reduce the cytotoxicity of PBAE/pEGFP polycomplex. However, MTX-PL/PBAE/pEGFP nanoparticles showed a remarkably increased cytoxicity compared to both PBAE/pEGFP polycomplex and PL/PBAE/pEGFP nanoparticles, e.g., only 26.5% of the cells survived at PBAE concentration of 100 μg/mL (Figure 6a). The above results indicated that MTX-PL/PBAE/pEGFP nanoparticles had a significant inhibitory effect on the proliferation of HepG2 cells. Moreover, we also evaluated the cytotoxicity of MTX-PL/PBAE/pEGFP nanoparticles in human normal liver HL-7702 cells. As shown in Figure S2, MTX-PL/PBAE/pEGFP nanoparticles had a significant inhibitory effect on the proliferation of human normal liver cells. It was thus deduced that MTX-PL/PBAE/pEGFP nanoparticles did not exhibit significant selectivity for the hepatoma at cellular level.

The mechanism of MTX-PL/PBAE/pEGFP nanoparticles on HepG2 cells is illustrated in Figure 6b. MTX-PL/PBAE/pEGFP nanoparticle first entered HepG2 cells through endocytosis mediated by ASGPR. Because of the the proton sponge effect and the pH-sensitive biodegradability of PBAE,[21−25] the particle core of PBAE/pEGFP polycomplex could promote endo/lysosomal disruption and gradually disintegrate with the increased acidity of endo/lysosomal compartment, thus triggering the escape of PBAE/pEGFP polycomplex and MTX-PL from endo/lysosome. After that, pEGFP was released into the cytoplasm and finally transported to the cell nucleus for expression of EGFP. MTX was released from MTX-PL through the esterase-catalyzed hydrolysis of ester bond in the cytoplasm to exert its therapeutic effect.

The above results have confirmed that MTX-PL could specifically bind to ASGPR on HepG2 cells (Figure 2). Next, we established a HCC xenograft mouse model using HepG2 cells, and then assessed the in vivo delivery of MTX-PL-Cy5.5 conjugate and MTX-PL-Cy5.5/PBAE/pEGFP nanoparticles after intravenous injections using in vivo imaging technique. The biodistribution of free Cy5.5 was first assessed. As shown in Figure S3, free Cy5.5 was rapidly eliminated from the body of the mouse, and its fluorescence signals completely disappeared at 24 h. However, MTX-PL-Cy5.5 was mainly distributed in the liver and the bladder at 1 h after administration, began to enter the tumor at 4 h, and was almost entirely accumulated in the liver and the tumor at 24 h (Figure 7a). It thus could be deduced that MTX-PL had the liver- and hepatoma-targeting capability due to its high affinity for ASGPR that is often overexpressed by the hepatocytes and hepatoma cells.[29−31] It was very exciting that MTX-PL-Cy5.5/PBAE/pEGPF nanoparticles exhibited more remarkable hepatoma-targeting property. After administration, MTX-PL-Cy5.5/PBAE/pEGFP nanoparticles were mainly located in the bladder at 1 h and began to be accumulated in the tumor at 4 h, and the fluorescent signal was observed only in the tumor at 24 h (Figure 7b). The further detection of major tissues showed that the fluorescent signal in the tumor was obviously stronger than that in the liver (Figure 7b). We believed this distinct hepatoma-targeting property was attributed to the following two factors. First, MTX-PL/PBAE/pEGFP nanoparticles had a small size below 200 nm and thus could take advantage of the enhanced permeability and retention (EPR) effect to accumulate in the tumor tissue. Second, MTX-PL was a specific ligand of ASGPR and therefore could selectively accumulate in the tumor via specific ligand/receptor binding.

CONCLUSIONS

In this study, a novel nanoparticle carrier was designed based on pullulan and PBAE for the hepatoma-targeting codelivery of gene and chemotherapy agent. Model gene, pEGFP, was condensed with cationic PBAE to form PBAE/pEGFP polycomplex. MTX-PL, synthesized by covalent conjugation of MTX to pullulan, was then coated on the surface of PBAE/pEGFP polycomplex by adsorption, thus realizing the coloading of gene and chemotherapy agent. MTX-PL/PBAE/pEGFP nanoparticles exhibited significant synergic effects on hepatoma HepG2 cells, e.g., a high gene transfection capability that was comparable with PEI and a significantly enhanced cytotoxicity compared to PBAE/pEGFP polycomplex. In addition, MTX-PL/PBAE/pEGFP nanoparticles showed a strong hepatoma-targeting property at both cellular and animal levels. In conclusion, this novel nanoparticle delivery system had great potential for combination of gene therapy and chemotherapy.

ASSOCIATED CONTENT

Supporting Information

Additional experimental details and figures, synthesis and characterization of PBAE, the cytotoxicity of MTX-PL/PBAE/pEGF nanoparticles in HL-7702 cells, and biodistributions of free Cy5.5 in HepG2 tumor-bearing nude mouse. This material is available free of charge via the Internet at http://pubs.acs.org.

AUTHOR INFORMATION

Corresponding Authors

*N.Z.: e-mail, zhangning@tijmu.edu.cn.
*Y.W.: e-mail, wangyinsong@tijmu.edu.cn.

Author Contributions

§Y.L. and Y.W. contributed equally.

Notes

The authors declare no competing financial interest.

ACKNOWLEDGMENTS

This research was supported by the 973 program (Grant 2011CB933100), National Natural Science Foundation of China (Grant 81371671), and National Science Fund for Distinguished Young Scholars (Grant 81125019).

REFERENCES

(1) Parkin, D. M.; Bray, F.; Ferlay, J.; Pisani, P. Estimating the World Cancer Burden: Globocan 2000. *Int. J. Cancer* **2001**, *94*, 153−156.

(2) Altekruse, S. F.; McGlynn, K. A.; Reichman, M. E. Hepatocellular Carcinoma Incidence, Mortality, and Survival Trends in the United States from 1975 to 2005. *J. Clin. Oncol.* **2009**, *27*, 1485−1491.

(3) Lau, W.-Y; Lai, E. C. H. Hepatocellular Carcinoma: Current Management and Recent Advances. *Hepatobiliary Pancreatic Dis. Int.* **2008**, *7*, 237−257.

(4) Blum, H. E. Hepatocellular Carcinoma: Therapy and Prevention. *World J. Gastroenterol.* **2005**, *11*, 7391−7400.

(5) Cahill, B. A.; Braccia, D. Current Treatment for Hepatocellular Carcinoma. *Clin. J. Oncol. Nurs.* **2004**, *8*, 393−399.

(6) Decadt, B.; Siriwardena, A. K. Radiofrequency Ablation of Liver Tumors: Systematic Review. *Lancet Oncol.* **2004**, *5*, 550−560.

(7) Ishikawa, H.; Nakao, K.; Matsumoto, K.; Ichikawa, T.; Hamasaki, K.; Nakata, K.; Eguchi, K. Antiangiogenic Gene Therapy for Hepatocellular Carcinoma Using Angiostatin Gene. *Hepatology* **2003**, *37*, 696−704.

(8) Hwang, L.-H. Gene Therapy Strategies for Hepatocellular Carcinoma. *J. Biomed. Sci.* **2006**, *13*, 453−468.

(9) Hernández-Alcoceba, R.; Sangro, B.; Prieto, J. Gene Therapy of Liver Cancer. *Ann. Hepatol.* **2007**, *6*, 5−14.

(10) McMenamin, M. M. Translational Benefits of Gene Therapy to Date. *Clin. Oncol. Cancer Res.* **2011**, *8*, 10−15.

(11) Xu, Q.; Leong, J.; Chua, Q. Y.; Chi, Y. T.; Chow, P. K.; Pack, D. W.; Wang, C. H. Combined Modality Doxorubicin-Based Chemotherapy and Chitosan-Mediated p53 Gene Therapy Using Double-Walled Microspheres for Treatment of Human Hepatocellular Carcinoma. *Biomaterials* **2013**, *34*, 5149−5162.

(12) Jacobs, F.; Gordts, S. C.; Muthuramu, I.; Geest, B. D. The Liver as a Target Organ for Gene Therapy: State of the Art, Challenges, and Future Perspectives. *Pharmaceuticals* **2012**, *5*, 1372−1392.

(13) Thomas, C. E.; Ehrhardt, A.; Kay, M. A. Progress and Problems with the Use of Viral Vectors for Gene Therapy. *Nat. Rev. Genet.* **2003**, *4*, 346−358.

(14) Kaufmann, K. B.; Büning, H.; Galy, A.; Schambach, A.; Grez, M. Gene Therapy on the Move. *EMBO Mol. Med.* **2013**, *5*, 1642−1661.

(15) Niidome, T.; Huang, L. Gene Therapy Progress and Prospects: Nonviral Vectors. *Gene Ther.* **2002**, *9*, 1647−1652.

(16) Zhang, Y.; Satterlee, A.; Huang, L. In Vivo Gene Delivery by Nonviral Vectors: Overcoming Hurdles? *Mol. Ther.* **2012**, *20*, 1298−1304.

(17) Ding, B.; Li, T.; Zhang, J.; Zhao, L.; Zhai, G. Advances in Liver-Directed Gene Therapy for Hepatocellular Carcinoma by Non-Viral Delivery Systems. *Curr. Gene Ther.* **2012**, *12*, 92−102.

(18) Morille, M.; Passirani, C.; Vonarbourg, A.; Clavreul, A.; Benoit, J.-P. Progress in Developing Cationic Vectors for Non-Viral Systemic Gene Therapy against Cancer. *Biomaterials* **2008**, *29*, 3477−3496.

(19) Canine, B. F.; Hatefi, A. Development of Recombinant Cationic Polymers for Gene Therapy Research. *Adv. Drug Delivery Rev.* **2010**, *62*, 1524−1529.

(20) Ibraheem, D.; Elaissari, A.; Fessi, H. Gene Therapy and DNA Delivery Systems. *Int. J. Pharm.* **2014**, *459*, 70−83.

(21) Anderson, D. G.; Peng, W.; Akinc, A.; Hossain, N.; Kohn, A.; Padera, R.; Langer, R.; Sawicki, J. A. A Polymer Library Approach to Suicide Gene Therapy for Cancer. *Proc. Natl. Acad. Sci. U.S.A.* **2004**, *101*, 16028−16033.

(22) Green, J. J.; Chiu, E.; Leshchiner, E. S.; Shi, J.; Langer, R.; Anderson, D. G. Electrostatic Ligand Coatings of Nanoparticles Enable Ligand-Specific Gene Delivery to Human Primary Cells. *Nano Lett.* **2007**, *7*, 874−879.

(23) Lee, J.-S.; Green, J. J.; Love, K. T.; Sunshine, J.; Langer, R.; Anderson, D. G. Gold, Poly(α-amino ester) Nanoparticles for Small Interfering RNA Delivery. *Nano Lett.* **2009**, *9*, 2402−2406.

(24) Fields, R. J.; Cheng, C. J.; Quijano, E.; Weller, C.; Kristofik, N.; Duong, N.; Hoimes, C.; Egan, M. E.; Saltzman, W. M. Surface Modified Poly(β amino ester)-Containing Nanoparticles for Plasmid DNA Delivery. *J. Controlled Release* **2012**, *164*, 41−48.

(25) Gu, J.; Wang, X.; Jiang, X.; Chen, Y.; Chen, L.; Fang, X.; Sha, X. Self-Assembled Carboxymethyl Poly(L-histidine) Coated Poly(β-amino ester)/DNA Complexes for Gene Transfection. *Biomaterials* **2012**, *33*, 644−658.

(26) Leathers, T. D. Biotechnological Production and Applications of Pullulan. *Appl. Microbial. Biotechnol.* **2003**, *62*, 468−473.

(27) Singha, R. S.; Sainia, G. K.; Kennedy, J. F. Pullulan: Microbial Sources, Production and Applications. *Carbohydr. Polym.* **2008**, *73*, 515−531.

(28) Moghimi, S. M.; Hunter, A. C.; Murray, J. C. Long-Circulating and Target-Specific Nanoparticles: Theory to Practice. *Pharmacol. Rev.* **2001**, *53*, 283−318.

(29) Kaneo, Y.; Tanaka, T.; Nakano, T.; Yamaguchi, Y. Evidence for Receptor-Mediated Hepatic Uptake of Pullulan in Rats. *J. Controlled Release* **2001**, *70*, 365−373.

(30) Tang, H.-B.; Li, L.; Chen, H.; Zhou, Z.-M.; Chen, H.-L.; Li, X.-M.; Liu, L.-R.; Wang, Y.-S.; Zhang, Q.-Q. Stability and in Vivo Evaluation of Pullulan Acetate as a Drug Nanocarrier. *Drug Delivery* **2010**, *17*, 552−558.

(31) Wang, Y.; Chen, H.; Liu, Y.; Wu, J.; Zhou, P.; Wang, Y.; Li, R.; Yang, X.; Zhang, N. pH-Sensitive Pullulan-Based Nanoparticle Carrier of Methotrexate and Combretastatin A4 for the Combination Therapy against Hepatocellular Carcinoma. *Biomaterials* **2013**, *34*, 7181−7190.

(32) Hossain, M. A.; Kim, D. H.; Jang, J. Y.; Kang, Y. J.; Yoon, J.-H.; Moon, J.-O.; Chung, H. Y.; Kim, G.-Y.; Choi, Y. H.; Copple, B. L.; et al. Aspirin Induces Apoptosis in Vitro and Inhibits Tumor Growth of Human Hepatocellular Carcinoma Cells in a Nude Mouse Xenograft Model. *Int. J. Oncol.* **2012**, *40*, 1298−1304.

(33) Davis, B. G.; Robinson, M. A. Drug Delivery Systems Based on Sugar-Macromolecule Conjugates. *Curr. Opin. Drug Discovery Dev.* **2002**, *5*, 279−288.

(34) Medina, S. H.; Tekumalla, V.; Chevliakov, M. V.; Shewach, D. S.; Ensminger, W. D.; El-Sayed, M. E. H. *N*-Acetylgalactosamine-Functionalized Dendrimers as Hepatic Cancer Cell-Targeted Carriers. *Biomaterials* **2011**, *32*, 4118−4129.

(35) Guo, R.; Yao, Y.; Cheng, G.; Wang, S. H.; Li, Y.; Shen, M.; Zhang, Y.; Baker, J. R.; Wang, J.; Shi, X. Synthesis of Glycoconjugated Poly(amindoamine) Dendrimers for Targeting Human Liver Cancer Cells. *RSC Adv.* **2012**, *2*, 99−102.

(36) Nishida, K.; Eguchi, Y.; Takino, T.; Takakura, Y.; Hashida, M.; Sezaki, H. Hepatic Disposition Characteristics of ^{111}In-Labeled Lactosaminated Bovine Serum Albumin in Rats. *Pharm. Res.* **1991**, *8*, 1253−1257.

(37) Grandinetti, G.; Smith, A. E.; Reineke, T. M. Membrane and Nuclear Permeabilization by Polymeric pDNA Vehicles: Efficient Method for Gene Delivery or Mechanism of Cytotoxicity? *Mol. Pharmaceutics* **2012**, *9*, 523−538.

(38) Fischer, D.; Li, Y.; Ahlemeyer, B.; Krieglstein, J.; Kissel, T. In Vitro Cytotoxicity Testing of Polycations: Influence of Polymer Structure on Cell Viability and Hemolysis. *Biomaterials* **2003**, *24*, 1121−1131.